PRELIMINARY RESULTS FROM THE RAIN MESOSPHERIC AND STRATOSPHERIC AEROSOL PARTICLE COLLECTION EXPERIMENT LAUNCHED ON REXUS-11

Patrick Magnusson[1], William Reid[1], Peggy Achtert[2], Nickolay Ivchenko[1], Erik Lindén[1], Valeriy Shepenkov[3], and Gunnar Tibert[3]

[1]*Space and Plasma Physics, School of Electrical Engineering, Royal Institute of Technology (KTH), SE-100 44 Stockholm, Sweden, Email: nickolay@kth.se*
[2]*Department of Meteorology, Stockholm University, SE-106 91 Stockholm, Sweden, Email: gunnar.tibert@mech.kth.se*
[3]*Department of Mechanics, Royal Institute of Technology (KTH), SE-100 44 Stockholm, Sweden, Email: peggy@misu.su.se*

ABSTRACT

The RAIN (Rocket deployed Atmospheric probes conducting Independent measurements in Northern Sweden) experiment demonstrates a technique for collecting aerosol particles in the middle atmosphere using multiple probes ejected from a sounding rocket. Collection samples on each probe are exposed over varying height ranges between 80 and 22 km giving an altitude distribution profile of aerosol particles. The experiment was launched on board the REXUS-11 sounding rocket on November 16, 2012 from Esrange Space Centre. The experiment operated nominally and was recovered. Initial scanning electron microscopy analysis of the collection samples indicates that aerosols were collected during the fall, however detailed analysis over all height ranges is ongoing.

1. INTRODUCTION

The influence of middle-atmospheric aerosol on climate variability is not yet fully understood. It is known that the stratospheric aerosol extends between the tropopause to about 30 km and is dominated by sub-micrometer hydrate sulphuric acid droplets which scatter incident sunlight [1]. It is also known that the upper-mesosphere aerosol is dominated by meteoric material that enters the earth's atmosphere and forms nanometer sized particles. These nanometer sized meteoric particles influence several middle-atmospheric processes, such as noctilucent clouds (NLCs), polar mesospheric summer echoes (PMSEs), metal layers and the heterogeneous chemistry that controls the budget of key species like water vapour [2; 3; 4; 5].

The size range and the concentration of stratospheric aerosols have previously been characterised by balloon-borne measurements [6], lidar [7] and satellite observations [8]. The size and composition of particles in NLCs has been monitored by satellite-based instruments [9] and ground-based instruments [10], but the microphysical properties of meteoric-smoke particles are still poorly understood. This is due to the the complications involved with in situ measurements at mesospheric altitudes. These measurements have only been performed by experiments on board sounding rockets [11], and the capturing of nanometer-sized particles is constrained by the shock wave in front of the rocket [12] and by contamination from the rocket itself.

A new method for collecting middle-atmospheric aerosols that involves free falling probes that are ejected from a sounding rocket is described. The experiment is called RAIN (Rocket deployed Atmospheric probes conducting Independent measurements in Northern Sweden). Two free falling aerosol collection probes are deployed from a sounding rocket and collect aerosol particles over varying height ranges between altitudes of 80 and 22 km. By using multiple probes independent of the rocket, the risk of contamination of the collected samples from the rocket is reduced and horizontal aerosol distributions at similar altitudes can also be studied. This paper outlines the design of the experiment in Section 2, the experiment results in Section 3 and a discussion of the results and further work in Section 4.

2. EXPERIMENT DESIGN

The planned flight timeline is summarised in Fig. 1. At 63 km altitude and t+67 s, the aerosol collection probes or free falling units (FFUs) are deployed from the rocket. The FFUs rise to an apogee of 85 km at t+145 s and activate their aerosol collection experiments (ACEs). Aerosol collection continues until the FFUs fall to an altitude of 17 km at t+285 s. At 6 km, a pressure sensor on each FFU triggers deployment of a parachute. During controlled descent each FFU broadcasts its GPS coordinates via a VHF radio transmission and satellite messages. After landing, the FFUs continue to transmit their positions, at which point a helicopter recovery crew lo-

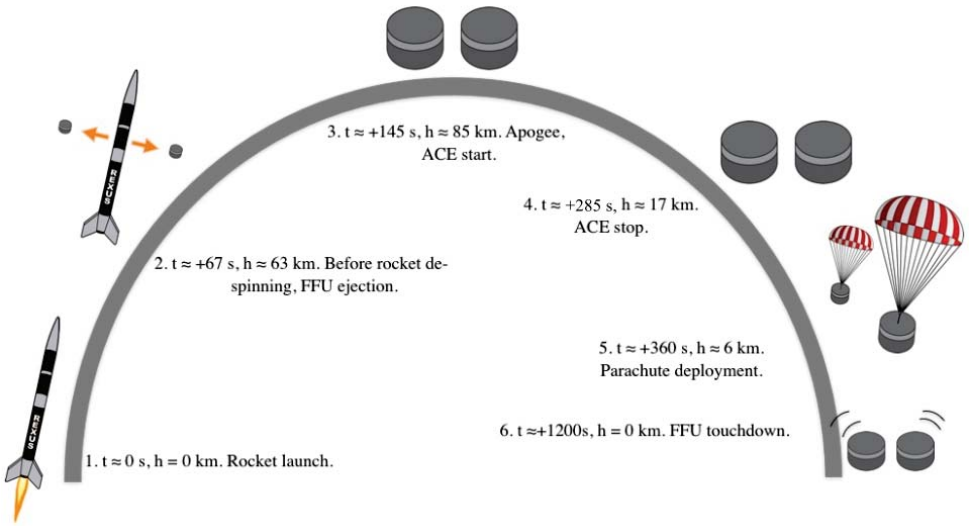

Figure 1. The flight timeline for the RAIN experiment.

cates and collects both units.

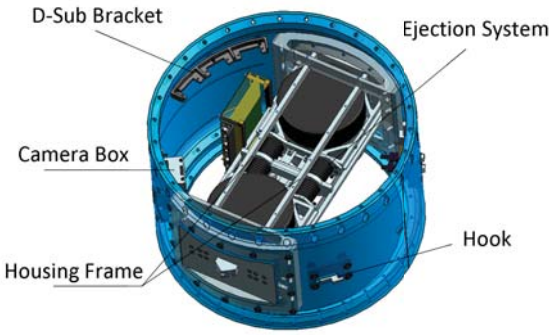

Figure 2. The Rocket Mounted Unit (RMU) that contains the two Free Falling Units up until the point of ejection. Ejection is triggered by a steel cable routed around the outside of the RMU being cut and the four 215 N compression springs pushing the FFUs out. A baffle over the hook and curved hatches was later added to protect the cable from the airflow.

The RAIN experiment consists of two parts: the rocket mounted unit (RMU) and the aerosol collecting FFUs. The RMU consists of a spring based ejection system, a camera and electronics used to charge and communicate with the FFUs. A labelled view of the RMU is shown in Fig. 2. The ejection system is a spring-based system that uses four 215 N compression springs. The FFUs are held within an ejection system housing made up of six aluminium bars. These bars are held inside two D-shaped mounts that are attached to the surface of the rocket cylinder. The mounts have been designed as reinforcements for the rocket cylinder structure so that the ejection hatches cut out of the cylinder do not detrimentally affect the rockets structural integrity. Each FFU is surrounded by a push plate. Each push plate takes the load of two compressed ejection springs while the system is in its loaded state. When the ejection springs are released the push plates slide along the ejection system housing bars, pushing the FFUs out of the rocket. On the opposite side of the FFU is a hatch assembly. The hatch interfaces with the push plates so that the force of the compressed springs is transmitted to it instead of the FFU. A 2 mm thick steel cable is routed around the circumference of the rocket cylinder and constrained at its two ends to hold the ejection springs in their compressed state. The termination of the cable has an eyelet that is placed onto the hook. The other end of the cable is held inside the rocket cylinder between two ruffled steel blocks that are bolted together. Before being placed between these steel blocks, the cable is passed through a pyrotechnic cutter that is used to cut the cable at ejection. To protect against localised heating in the airflow, the cable eyelet on the hook is shielded by a baffle.

The FFU is divided into three parts: the recovery system, the electronics system and the ACE as presented in Fig. 3. The recovery system consists of a parachute, the FFU hat and a release system for the hat. When the FFU falls past 6 km, a thermal cutter burns through a fishing line, releasing clamps that hold the FFU hat and the parachute is deployed. The electrical system's role is to control the release of the parachute at the correct altitude, operate the localisation system, collecting housekeeping and GPS data, control the ACE and allow communication with the RMU. The localisation system consists of a commercial GPS, a radio beacon and a satellite modem to send out the position of the FFU via both the beacon and the satellite modem.

The ACE is composed of a collection plate gear loaded with aerosol collection samples and the FFU's bottom plate, which has an exposure window in it. The gear is ro-

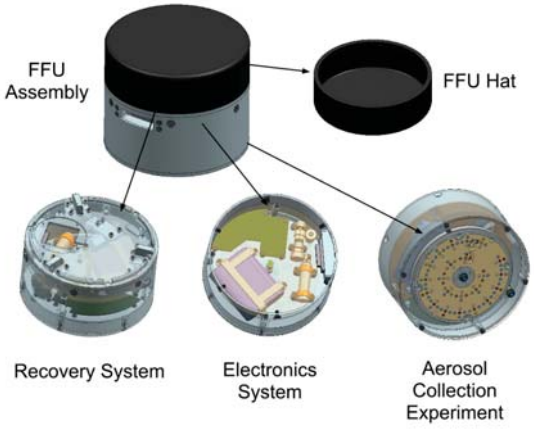

Figure 3. The FFU consists of a recovery system, electronic system and an aerosol collection experiment.

tated past the exposure window, exposing different samples at different altitudes. To prevent contamination of the samples, a seal is created between the collection plate and the FFU base plate by pressing the surfaces coated with teflon coated covered glass fibre against each other with a spring washer. The positioning of the 110 collection samples, each 3 mm in diameter, within the collection plate is presented in Fig. 4. Also shown are the positions of the different types of collection samples used. The first three are different types of standard transmission electron microscopy (TEM) grids: formvar/carbon 400 mesh, ultrathin carbon type-A 400 mesh, and ultrathin carbon film on holey carbon support film 400 mesh. The last two materials are glass fibre and silicone gel. The samples are placed in sample holders containing five samples each. The sample holders can easily be removed and directly put in to a scanning electron microscope (SEM) for analysis. The samples are arranged into six rows and 48 columns as presented in Fig. 4 where row one and six contain control samples and are not exposed to the atmosphere. A more detailed description of the experiment design is available in [13].

3. RESULTS

The RAIN experiment was launched onboard the REXUS-11 sounding rocket from Esrange Space Centre in Kiruna, Sweden at 11:45 (UTC+1) on November 16, 2012. All phases of the flight except for parachute deployment were executed according to the plan presented in Fig. 1 with minor altitude differences. The following section features a reconstruction of the RAIN flight using rocket and FFU sensor data and presents preliminary results from analysis of the ACE. The two flight units are identified as FFU C and FFU E.

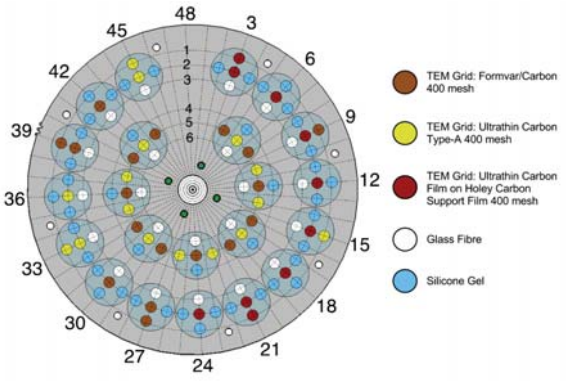

Figure 4. The ACE collection plate gear contains 110 collection samples. Rows 2,3,4 and 5 are directly exposed to the airflow while rows 1 and 6 contain control samples.

3.1. Flight Reconstruction

From the collected raw GPS data that were processed post-flight, the vertical velocity and altitude is presented in Fig. 5. The FFUs were ejected at 57 km and reached an apogee of 78.5 km. The ACEs were activated at apogee and stopped at 22 km. FFU E's parachute was prematurely deployed at 13 km, while FFU C's parachute was prematurely deployed at 10 km. At ejection, the vertical velocity of the FFUs were 630 m/s. The velocity then decreased linearly until the FFUs reached a minimum vertical velocity of -730 m/s before the FFUs underwent maximum braking due to atmospheric drag. After parachute deployment the velocity reduced to 11 m/s.

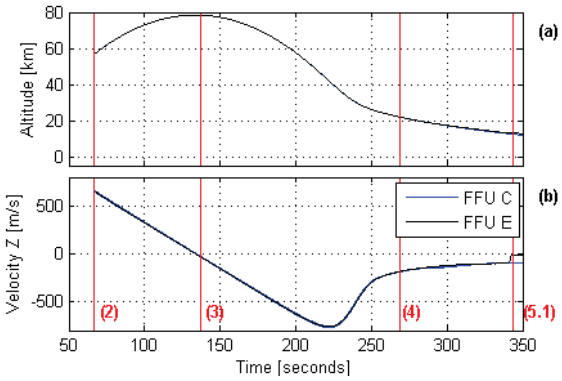

Figure 5. The altitude and velocity in the vertical direction of the two FFUs from ejection, (2), to the premature parachute deployment of FFU E, (5.1). Start of aerosol collection is at (3) and stop of aerosol collection is at (4).

The FFU ejection system operated nominally, however the ejection dynamics between each FFU had slight differences. FFU C was deployed at a speed of 5 m/s, while FFU E was deployed with a velocity magnitude of 6.5 m/s as shown in Fig. 6. In addition, the angle between the FFUs' velocity vectors is not 180° as presented in Fig. 6 and Fig. 7. It is therefore known that the FFUs were not

deployed symmetrically, and that FFU C was deployed slightly later than FFU E. All of these behaviours can be attributed to the ejection constraint cable impeding the ejection of FFU C more than FFU E. The ejection cable is cut next to FFU E's ejection hatch, while the other end of the cable is constrained next to the FFU C ejection hatch. This results in the cable taking a longer time to come free of the rocket cylinder surface on the FFU C side, thereby impeding the ejection of FFU C.

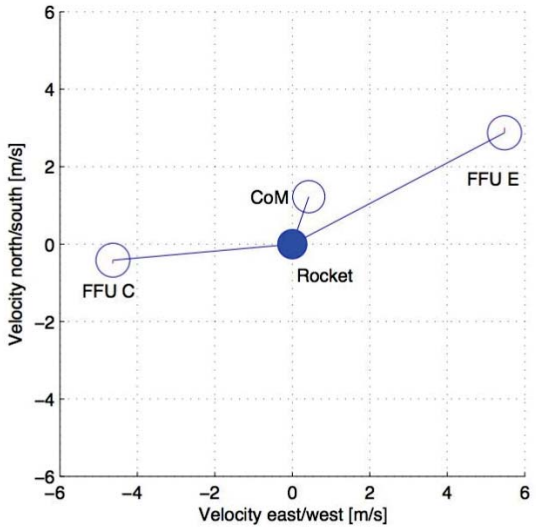

Figure 6. The velocity vectors of the FFUs 1.5 seconds after ejection from the rocket. The centre of mass of the two FFUs and its velocity vector is also shown.

Even though an asymmetric ejection was observed, the ejection system was able to fulfil its two operational requirements of ejecting the two FFUs with a velocity greater than or equal to 5 m/s, and ejecting them so that they fell with their base plates facing towards the Earth. In Fig. 8 it is shown that as the FFUs fell, they precessed for the duration of the ACE, with the FFU base plates facing into the air stream.

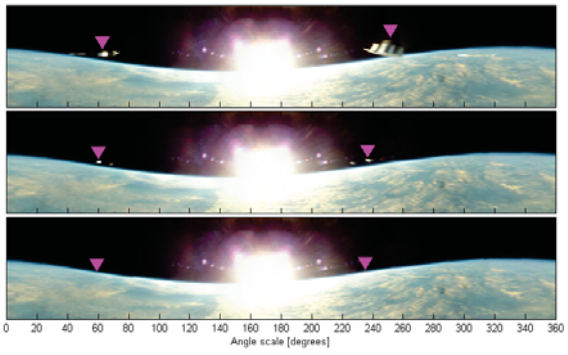

Figure 7. A panoramic view of the two FFUs leaving the rocket during the three rotations of the rocket directly after ejection.

From the vertical axis accelerometer data, presented in Fig. 8 (a), it is possible to see the acceleration increase during the peak braking which indicates that the FFU was falling with its base plate facing towards the Earth. After the aerosol collection stops, the FFU starts to autorotate, and shortly after the hats are ripped off the FFUs and the parachutes are deployed. The angular rate around the vertical axis is presented in Fig. 8 (b) and shows an interesting phenomenon at ejection where the angular rate is reduced from 3.3 Hz to 1.8 Hz for each FFU. From the angular rates of all three axes, presented in Fig. 8(b)-(d), it is observed that the angular momentum is not conserved and therefore an external torque is present during ejection. Even if the angular rate about the vertical axis decreases they are still spinning and stabilised, falling with the bottom plates facing down. The FFUs also start to precess after ejection. From Fig. 8(c)-(d) it is observed that FFU C has a larger precession than FFU E.

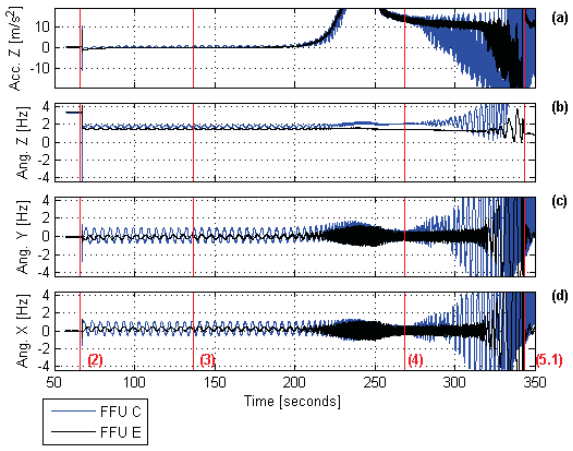

Figure 8. The acceleration in Z-direction and angular rate in all three axes for the two FFUs measured with the internal sensors. The ejection from the rocket is at 67 s marked with (2), the ACE starts at (3) and stops at (4) and the parachute deployment for FFU E occurs at (5.1).

The pressure, temperature, and battery voltage from launch to landing are presented in Fig. 9 (a)-(c). The pressure decreases below the pressure sensors' measurement range approximately 20 s after launch. The pressure then starts to increase exponentially before parachute deployment at (5.1) for the parachute deployment of FFU E. The pressure then increased almost linearly as the FFUs had lower descent speed after the parachute deployment. The temperature inside the FFUs, presented in Fig. 9(b), increases when the FFU goes into vacuum and when the FFU reaches its terminal velocity. After parachute deployment, the temperature decreases to a minimum of -13.3° for FFU C and -19.2° for FFU E. The temperature then increased and did not vary much after landing, (6.2) and (6.1). In Fig. 9 (c) the battery voltage is presented. When the FFUs are in the rocket, the RMU supplies power to the FFUs and after ejection, (2), the FFUs then start to draw power from their internal batteries, indicated by a slight voltage drop. When the the

motor starts and aerosol collection begins, it is possible to see the battery voltages decrease. At 513 s after launch the thermal cutter is activated, which was supposed to deploy the parachute. The clamps are released but the top hat had already been torn off by the turbulent fall earlier. At ∼570 s the FFUs start to send out their GPS positions through the beacons and satellite modems. The dips in the battery voltages are the satellite modems trying to send messages. A strong dependence can be seen between the battery voltage in Fig. 9(c) and the temperature in Fig. 9(b) where the battery voltage decreases when the temperature decreases. The critical voltage level for the FFU batteries is 2.2 V. Throughout the flight and recovery, the FFU batteries were in no risk of reaching this low voltage level.

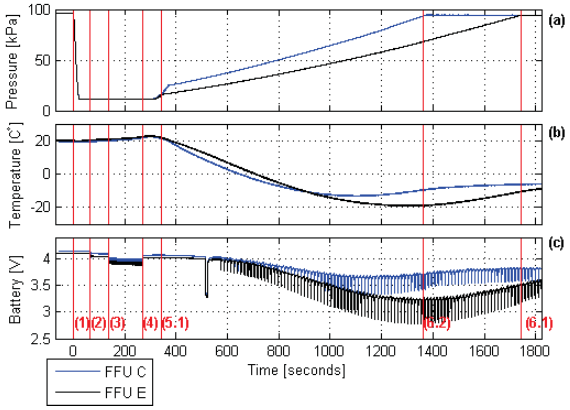

Figure 9. The measured pressure, battery voltage and temperature from launch to landing for FFU E in black and FFU C in blue. The ejection from the rocket is at 67 s at (2), the ACE starts at (3) and stops at (4), the parachute deployment for FFU E occurs at (5.1), landing for FFU E occurs at (6.1) and for FFU C the landing occurs at (6.2).

The localisation system worked and beacon messages were constantly received during the fall from 10 km to 800 m for FFU E and 7.7 km to 900 m for FFU C. Satellite modem messages were received at lower altitudes, and messages were successfully sent from the two landing sites. The FFU E drifted along a 25 km ground track and FFU C drifted along 17 km ground track from where the parachutes were deployed.

3.2. Aerosol Collection

From mapping the position of the aerosol collection plate to the altitude data it can be seen that each FFU exposed its aerosol collection samples to the airflow between 80 and 22 km. Fig. 10 shows the altitude ranges that each aerosol collection sample in FFU C were exposed to. The X axes show the collection plate column number presented in Fig. 4, while the Y axes show altitude. The four plots show exposure altitude ranges for each of the four rows exposed to the airflow. Row one and six were not exposed as they contain control samples.

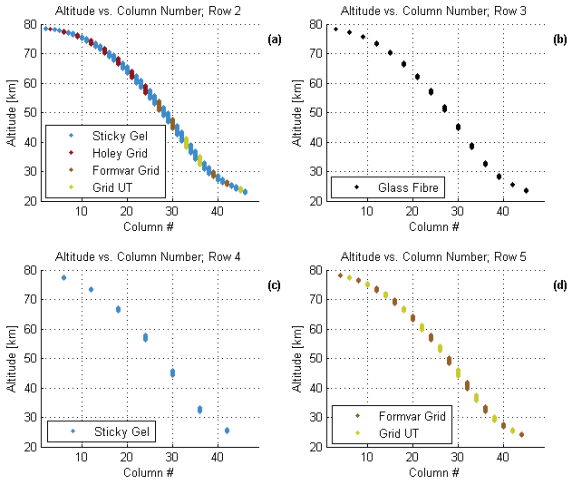

Figure 10. The altitude versus the exposed samples for row 2,3,4 and 5 for FFU C. Rows 1 and 6 are not exposed but contain control samples.

In an effort to prevent contamination the aerosol collection samples were loaded into the FFUs in a clean room. Before flight, the FFUs were cleaned using an ultrasonic bath and then wiped with isopropyl alcohol. The FFUs were stored and transported in sealed containers. After flight, FFU C was unpacked, while FFU E is still sealed and will be opened when analysis of FFU C is completed. Fig. 11 shows images of the FFU C collection plate and collection plate lid in an unpacked state post-flight. It is observed that approximately half of the aerosol collection sample holders became stuck in collection plate lid in Fig. 11 (b). It can also be seen that some of the copper grids stuck to the surface of the collection plate lid as opposed to staying in their collection sample holders. This is seen as an inconvenience when handling the samples given that more care has to be taken when removing the samples and preparing them for SEM and TEM analysis.

Preliminary SEM and X-ray material composition analysis of two silicone gel samples from FFU C is shown in Fig. 12. These two samples were selected because they were exposed at relatively low altitudes and therefore the probability of large particles being present is high. Sample C 239 was exposed over an altitude range between 30 km and 28 km, while sample C 241 was exposed between 29 km and 27 km. In image (b) a 50 μm by 30 μm feldspar particle is shown. In image (c) an unknown particle 40 μm wide and 100 μm particle is shown, however the composition for this particle is unresolved. In image (e) a 100 μm by 1000 μm quartz particle with tendrils is observed. These tendrils are assumed to be from a neighbouring glass fibre sample. Image (f) shows a 4 μm by 2 μm particle impact crater.

These preliminary results show that particles have been collected by at least two of the aerosol collection sam-

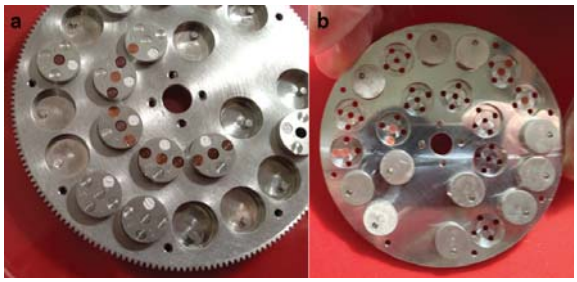

Figure 11. Images of the FFU C's collection plate (a) and collection plate lid (b) after flight. Half of the aerosol collection sample holders became stuck in the collection plate lid (b). In addition, seven TEM grids stuck to the collection plate lid in stead of staying in their collection sample holders. This will result in more complicated handling procedures for these samples.

ples. It is still necessary to determine if contaminants were introduced to the samples by analysing the control samples from rows 1 and 6. If it is shown that minimal contamination occurred then samples from different altitude ranges will be imaged to determine the specific altitude ranges over which particles were collected. Particle composition and concentration will also be investigated.

4. DISCUSSION

The RAIN experiment was successful in that it achieved all of its operational objectives. The premature deployment of the parachutes was the only unplanned event and did not detrimentally affect the performance of the experiment. The aerosol collection plates were exposed to the airflow according to plan, and the samples were exposed over an altitude range between 80 km and 22 km. During the aerosol collection the FFUs' underwent precession, however the base plates were facing the Earth's surface. Initial analysis shows that the FFUs collected aerosols but further analysis is needed to determine if the samples have been contaminated.

The ejection system for the FFUs was also proven to work, though the spin rate was reduced about the vertical axis quite substantially and the cause is yet to be determined. The cause of the asymmetric ejection angle between the FFUs is also being investigated.

The experiment demonstrated a GPS raw data collection technique. The GPS data were processed post-flight to find the ejection velocities and the positions of the FFUs which has been used to map each exposed aerosol collection sample to a height range. This proven GPS collection technique was used more recently with the KTH MUSCAT experiment and will be employed in future experiments run by the Space and Plasma Physics Department at the Royal Institute of Technology (KTH).

Possible experiment improvements include sub-system

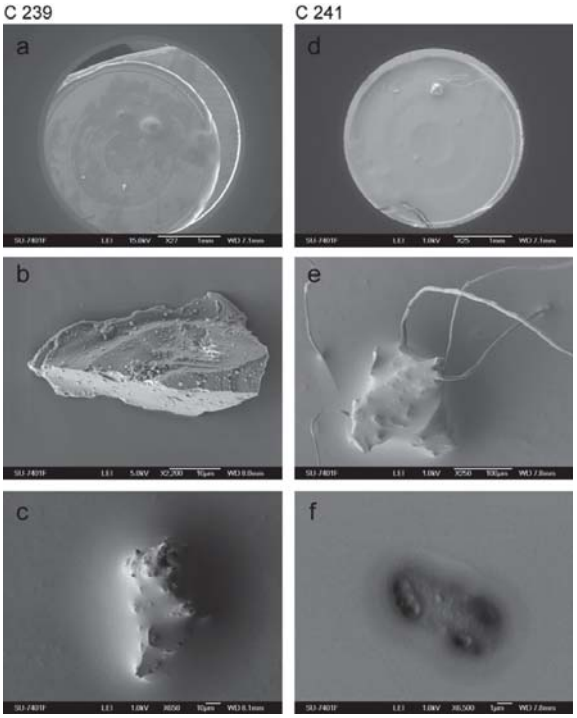

Figure 12. SEM images of two silicone gel samples from FFU C. Images (a) and (d) show overview images of the 3 mm diameter collection samples. Images (b),(c),(e) and (f) show particles or evidence of particles on the order of 10 μm in size.

re-designs within the RMU ejection system, the FFU recovery system and ACE. To perform a more symmetric ejection it is recommended that the ejection system cut the steel constraint cable at the two ends of the cable as opposed to just one. During the flight, the FFUs' recovery system top hats were ripped off while the FFUs were tumbling. To prevent this from happening again the recovery system can be modified so the lip in the interior of the top hat is wider and so the hooks can get a better grip and thus prevent strong loads from ripping off the hat. The ACE could be re-designed to prevent the aerosol collection sample holders from getting stuck in the collection plate lid. To solve this issue the tolerances for sample holder dimensions and the beds in which they sit inside the collection plate should be changed create a looser fit. Another design improvement would be making the aerosol collection sample holders usable in both scanning and transmission electron microscopes so as to prevent manipulation of individual aerosol collection samples. Currently, the design only allows for the collection sample holders to be used in scanning electron microscopy, and if it is desired to use the samples in a transmission electron microscope, then individual collection samples have to be removed from their holders and placed on another type of holder.

ACKNOWLEDGEMENTS

We would like to thank the entire RAIN team for all of the hard work and time they have contributed to this project. Team members include Tobias Kuremyr, Joakim Asplund, Axel Vidmark, Alexandra Oprea, Wenjie Jin, Baktash Samani, Sofhia Josborg, Martin Härberg, Roberto Chiarito, Daniel Brodén, Fredrik Backman, Oussama Chammam, Amer Halilovic, Kristoffer Hultgren, Adrian Ahmadi and Tobias Johansson. Thanks goes to the Swedish National Space Board and the German Aerospace Centre for making the REXUS program possible. The Swedish National Space Board also provided additional financial support to the RAIN experiment. The Swedish Space Corporation, the Mobile Rocket Base (MORABA) and the European Space Agency have been invaluable in their technical support. We would like to thank Kjell Jansson for his assistance with scanning electron microscopy analysis. We would also like to thank Space and Plasma Physics and the Department of Mechanics at KTH and the Stockholm University Meteorological Institute for all of their technical and financial support.

REFERENCES

[1] P. Hamill, E. Jensen, P. Russell, and J. Bauman, "The life cycle of stratospheric aerosol particles," *Bull. Am. Meteorol. Soc.*, vol. 78, pp. 1395–1410, 1997.

[2] R. Turco, O. Toon, R. Whitten, R. Keesee, and D. Hollenbach, "Noctilucent clouds: Simulation studies of their genesis, properties and global influences," *Planet. Space Sci.*, vol. 3, pp. 1147–1181, 1982.

[3] M. E. Summers and D. E. Siskind, "Surface recombination of O and H2 on meteoric dust as a source of mesospheric water vapor," *Geophys. Res. Lett.*, vol. 26, pp. 1837–1840, 1999.

[4] J. Plane, "The role of sodium bicarbonate in the nucleation of noctilucent clouds," *Ann. Geophys.*, vol. 18, pp. 807–814, 2000.

[5] L. Megner, D. Siskind, M. Rapp, and J. Gumbel, "Global and temporal distribution of meteoric smoke: A two-dimensional simulation study," *J. Geophys. Res.*, vol. 113, 2008.

[6] T. Deshler, M. Hervig, D. Hofmann, J. Rosen, and J. Liley, "Thirty years of in situ stratospheric aerosol size distribution measurements from Laramie, Wyoming (41°N), using balloon-borne instruments," *J. Geophys. Res.*, vol. 108(D22), 2003.

[7] H. Jager, "Long-term record of lidar observations of the stratospheric aerosol layer at Garmisch-Partenkirchen," *J. Geophys. Res.*, vol. 110, 2005.

[8] L. Thomason, L. Poole, and C. Randall, "Sticking efficiency of nanoparticles in high-velocity collisions with various target materials.," *Atmos. Chem. Phys.*, vol. 7, pp. 1423–1433, 2007.

[9] K. Pérot, A. Hauchecorne, F. Montmessin, J.-L. Bertaux, L. Blanot, F. Dalaudier, D. Fussen, and E. Kyrölä, "First climatology of polar mesospheric clouds from GOMOS/ENVISAT stellar occultation instrument," *Atmos. Chem. Phys.*, vol. 10, pp. 2723–2735, 2010.

[10] N. Kaifler, G. Baumgarten, J. Fiedler, R. Latteck, F.-J. Lübken, and M. Rapp, "Coincident measurements of PMSE and NLC above ALOMAR (69°N, 16°E) by radar and lidar from 1999–2008," *Atmos. Chem. Phys.*, vol. 11, pp. 1355–1366, 2011.

[11] J. Hedin, J. Gumbel, T. Waldemarsson, and F. Giovane, "The aerodynamics of the MAGIC meteoric smoke sampler," *Advances in Space Res.*, vol. 40, pp. 818–824, 2007.

[12] J. Hedin, J. Gumbel, and M. Rapp, "On the efficiency of rocketborne particle detection in the mesosphere," *Atmos. Chem. Phys.*, vol. 7, pp. 1183–1214, 2007.

[13] W. Reid, P. Achtert, N. Ivchenko, P. Magnusson, T. Kuremyr, V. Shepenkov, and G. Tibert, "A novel rocket-based in-situ collection technique for mesospheric and stratospheric aerosol particles," *Atmospheric Measurement Techniques Discussions*, vol. 5, p. 8161, 2012.